Published in final edited form as:
Circ Res. 2003 November 14; 93(10): e124–e135. doi:10.1161/01.RES.0000102404.81461.25.

ALDOSTERONISM AND PERIPHERAL BLOOD MONONUCLEAR CELL ACTIVATION: A NEUROENDOCRINE-IMMUNE INTERFACE

Robert A. Ahokas, PhD[*], **Kenneth J. Warrington, MD**[†], **Ivan C. Gerling, PhD**[‡], **Yao Sun, MD, PhD**[§], **Linus A. Wodi, MD**[§], **Paula A. Herring, MD**[†], **Li Lu, MD**[§], **Syamal K. Bhattacharya, PhD**[||], **Arnold E. Postlethwaite, MD**[†], and **Karl T. Weber, MD**[§]

[*] Department of Obstetrics & Gynecology, University of Tennessee Health Science Center, Memphis, Tennessee

[||] Department of Surgery, University of Tennessee Health Science Center, Memphis, Tennessee

[§] Division of Cardiovascular Diseases, University of Tennessee Health Science Center, Memphis, Tennessee

[†] Division of Connective Tissue Diseases, University of Tennessee Health Science Center, Memphis, Tennessee

[‡] Division of Endocrinology, Department of Medicine, University of Tennessee Health Science Center, Memphis, Tennessee

Summary

Aldosteronism eventuates in a proinflammatory/fibrogenic vascular phenotype of the heart and systemic organs. It remains uncertain whether peripheral blood mononuclear cells (PBMC) are activated prior to tissue invasion by monocytes/macrophages and lymphocytes as is the case for responsible pathogenic mechanisms. Uninephrectomized rats, treated for 4 wks with dietary 1%NaCl and aldosterone (0.75 μg/h, ALDOST) ± spironolactone (Spi, 100 mg/kg/daily gavage), were compared to unoperated/-untreated and uninephrectomized/salt-treated controls. Before intramural coronary vascular lesions appeared at wk 4 ALDOST, we found: 1) a reduction of PBMC cytosolic free $[Mg^{2+}]_i$, together with intracellular Mg^{2+} and Ca^{2+} loading while plasma and cardiac tissue Mg^{2+} were no different from controls; 2) increased H_2O_2 production by monocytes and lymphocytes together with upregulated PBMC gene expression of oxidative stress-inducible tyrosine phosphatase and Mn^{2+}-superoxide dismutase, and the presence of 3-nitrotyrosine in CD4+ and ED-1-positive inflammatory cells that had invaded intramural coronary arteries; 3) B cell activation, including transcription of immunoglobulins, ICAM-1, CC and CXC chemokines and their receptors; 4) expansion of B lymphocyte subset and MHC Class II-expressing lymphocytes; and 5) autoreactivity with gene expression for antibodies to acetylcholine receptors and a downregulation of RT-6.2, which is in keeping with cell activation and associated with autoimmunity. Spi co-treatment attenuated the rise in intracellular Ca^{2+}, the appearance of oxi/nitrosative stress in PBMC and invading inflammatory cells, and alterations in PBMC transcriptome. Thus, aldosteronism is associated with an activation of circulating immune cells induced by iterations in PBMC divalent cations and transduced by oxi/nitrosative stress. ALDO receptor antagonism modulates this neuroendocrine-immune interface.

Correspondence: Karl T. Weber, MD, University of Tennessee Health Science Center, Division of Cardiovascular Diseases, Rm 353 Dobbs Research Institute, 951 Court Ave. Memphis, TN 18163, Tel:901 448-5750 Fax: 901 448-8084, ktweber@utmem.edu.

Keywords

Aldosterone; Peripheral blood mononuclear cells; Cytosolic free Mg^{2+}; Cytosolic free Ca^{2+}; Oxi/nitrosative stress; Hydrogen peroxide production; Transcriptome

Introduction

Irrespective of its etiologic origins, asymptomatic ventricular systolic dysfunction eventuates in an activation of the circulating renin-angiotensin-aldosterone system (RAAS) whose effector hormones contribute to the appearance of the congestive heart failure (CHF) syndrome. A chronic systemic illness ensues that features: oxi/nitrosative stress in such diverse tissues as skeletal muscle, peripheral blood mononuclear cells (PBMC: monocytes and lymphocytes) and heart (1–11); elevated circulating levels of proinflammatory cytokines and chemokines (12–21); and a wasting syndrome that eventuates in cachexia (22). Pharmacologic modulation of RAAS effector hormones has proven clinical benefits in patients with CHF (23–27).

A role for angiotensin (Ang) II and aldosterone (ALDO) in the pathogenesis of the systemic illness that accompanies CHF is an area of ongoing research. A rodent model has been used to address the consequences of chronic inappropriate (relative to dietary Na^+ intake) elevations in plasma ALDO, comparable to those seen in human CHF. Treatment with ALDO and 1% dietary NaCl (ALDOST) rapidly suppresses plasma renin and AngII (28,29). At 4 wks ALDOST, coronary vascular lesions are first seen in the normotensive, nonhypertrophied right atrium and ventricle and left atrium, as well as in the hypertensive, hypertrophied left ventricle (30). Chronic mineralocorticoid excess, in combination with dietary salt excess and independent of blood pressure, is also known to adversely affect the structure of intramural arteries of systemic organs, including kidneys, pancreas and mesentery, which can be prevented by ALDO-receptor antagonist (31–40).

Commonly featured in coronary vascular lesions are inflammatory cells and myofibroblasts (28,30,41). In the monocytes/macrophages and lymphocytes that invade intramural coronary arteries, Sun et al. (42) found an induction of oxi/nitrosative stress and activation of a redox-sensitive nuclear transcription factor-κB (NFκB), together with upregulated mRNA expression of a proinflammatory mediator cascade that NFκB regulates. Co-treatment with either spironolactone (Spi), an ALDO receptor antagonist, or an antioxidant prevented these molecular events. Eplerenone, another ALDO receptor antagonist, is also cardioprotective in this model (43). This proinflammatory/fibrogenic cardiac phenotype is not seen with ALDO plus a 0.4% NaCl diet or with a 1% NaCl diet alone (44). Moreover, cardioprotective effects of ALDO receptor antagonism during ALDOST are seen with either nondepressor or depressor doses of Spi (45). The importance of ALDOST (vis-à-vis hemodynamic factors) in eliciting this phenotype has been demonstrated in multiple studies reported over the past decade (28, 38,39,41,42,45–48). Nevertheless, there are many gaps in our knowledge regarding the role of ALDO and Na^+ in the pathogenesis of coronary vascular remodeling. For example, whether immune cells are activated prior to tissue invasion? What accounts for the induction of oxi/nitrosative stress in these cells? Given that spironolactone abrogates these immune cell responses as recently reported (42), whether its mechanism of action is immodulatory remains to be determined.

A Na^+-dependent reduction in cytosolic free Mg^{2+} ($[Mg^{2+}]_i$) accompanies ALDO receptor-ligand binding in cultured human lymphocytes (49,50). Herein we hypothesized ALDOST leads to a reduction in PBMC $[Mg^{2+}]_i$, the biologically active component of this important intracellular divalent cation which, in turn, contributes to intracellular Ca^{2+} loading, the induction of oxi/nitrosative stress and immune cell activation prior to the appearance of the

proinflammatory coronary vascular phenotype. We further hypothesized Spi prevents these responses. Accordingly, blood was harvested weekly from uninephrectomized rats receiving ALDOST or ALDOST plus Spi for 4 wks. We monitored PBMC $[Mg^{2+}]_i$ and $[Ca^{2+}]_i$ and several indices of oxi/nitrosative stress that included: hydrogen peroxide (H_2O_2) generation by PBMC; differential expression of PBMC genes, including those related to oxi/nitrosative stress and antioxidant defenses; and circulating B and T lymphocyte responses. At wk 4, we examined coronal sections of right and left ventricles for the presence of 3-nitrotyrosine in inflammatory cells that invaded the coronary vasculature. Age-/gender-matched unoperated/untreated and uninephrectomized rats receiving a 1% NaCl diet served as control groups.

METHODS

Animals

Eight-week-old male Sprague-Dawley rats (Harlan, IN, USA) were used. The study was approved by the institution's Animal Care and Use Committee. Unoperated, untreated age-/gender-matched rats served as one control group (n=5). Uninephrectomized rats receiving 1% NaCl/0.4% KCl in drinking water and standard laboratory chow served as a second control group (n=10). Separate groups of uninephrectomized, salt-treated rats received ALDO (0.75μg/h) by implanted minipump (Alzet, Cupertino, CA, USA) for 1 to 4 wks (n=10 at each time point). This dose of ALDO promptly raises its plasma levels in rats to those seen in man with CHF. ALDOST rapidly suppresses plasma renin activity and circulating angiotensin II (28,29). A separate group of animals received ALDOST together with Spi (100 mg/kg by daily gavage). Animals were observed daily for their physical activity and consumption of food and water. Systolic blood pressure was recorded weekly as previously reported (28,42). At the conclusion of wks 1 to 4 of ALDOST and ALDOST + Spi, animals were weighed, anesthetized, blood collected by cardiac puncture and hearts harvested.

Plasma and Cardiac Tissue Mg^{2+} Concentrations

Plasma was diluted 1:20 with 0.5% lanthanum chloride and Mg^{2+} concentration was quantified in 100μL specimens employing a Varian model 220 FS double-beam fast sequential atomic absorption spectrophotometer (Varian Techtron, Melbourne, Australia) using a modification of the method of Bhattacharya (51). Plasma Mg^{2+} levels are expressed in mg/dL.

Microdetermination for Mg^{2+} concentration in ventricular myocardium was carried out in 12–15 mg demoisturized, defatted specimens, following complete digestion in 0.75 M Ultrex quality nitric acid (J. G. Baker Chemical Co., Phillipsburg, PA, USA) at 68°C for 15 hrs (52). This procedure has been shown to extract more than 99% of Mg^{2+} from dry, defatted tissue. Tissue Mg^{2+} levels are expressed in nEq/mg of fat-free dry tissue.

Isolation of PBMC

Heparinized whole blood (5–8 mL) was diluted to 10 mL with phosphate buffered saline (PBS, pH 7.4), layered on top of 5 mL Histopaque 1083 and centrifuged for 30 min at 400×*g*. PBMCs were aspirated, washed twice, suspended in PBS and counted with a hemocytometer.

Quantitation of Total Mg^{2+} and Ca^{2+} Concentration in PBMC

Isolated PBMCs were washed three times with 140 mM choline chloride. The PBMCs were then lysed with 2 mL deionized water and subjected to three cycles of alternate freezing at −70°C and thawing. An aliquot of 1.9 mL of isolated PBMC suspension containing 1–5 mg/mL protein was digested with 0.4 mL of 0.75 M Ultrex quality nitric acid (J. T. Baker, Phillipsburg, NJ, USA) for 24 hr at 68°C. The acid-extracted suspension was centrifuged, 1 mL of supernatant was diluted with 3 mL 0.5% $LaCl_3$ solution and the diluent used to quantitate

PBMC Mg^{2+} and Ca^{2+} levels by atomic absorption spectroscopy, as described elsewhere (52,53). The protein level in the PBMC suspension was assayed as previously described (54) and total Mg^{2+} and Ca^{2+} concentrations were expressed in μg/mg protein.

Cytosolic Free $[Mg^{2+}]_i$ and $[Ca^{2+}]_i$ in PBMC

Separate PBMC aliquots (1×10^6 cells) were loaded with the cell permeant fluorescent probes mag-fura-2 acetoxymethyl ester and fura-2 acetoxymethyl ester (Molecular Probes, Eugene, OR, USA) for the ratiometric measurement of $[Mg^{2+}]_i$ and $[Ca^{2+}]_i$, respectively, using a Perkin Elmer LS-50B spectrofluorometer (Shelton, CT, USA) according to the method of Delva et al. (50). After loading cells with mag-fura-2 and washing them, cells are suspended in a buffer containing Mg^{2+} for spectrofluorometric measurement. Some mag-fura-2 leaks back out of the cells and is available to react with extracellular Mg^{2+}. EDTA and EGTA are added to the suspension to chelate this extracellular Mg^{2+} so that only intracellular Mg^{2+}/mag-fura-2 fluorescence (or resting cytosolic ionized Mg^{2+}) is measured. As a result of this chelation of extracellular Mg^{2+}, there is a small decrease in fluorescence. It is this latter value, following the addition of EDTA and EGTA, which represents true cytosolic Mg^{2+} and which are reported herein. The measurement of Ca^{2+} reported herein likewise is made after addition of the chelator EGTA so that only true free cytosolic Ca^{2+} is measured. Specific details can be found elsewhere (55) and the online data supplement available at http://www.circresaha.org.

Hydrogen Peroxide Generation by PBMC

For the measurement of hydrogen peroxide (H_2O_2) production, 100μL aliquots of whole blood obtained serially from the same animals by cardiac punction were incubated with 2,7-dichlorofluorescein diacetate (25μM) for 45 min at 37°C. After lysing erythrocytes with FACS lysing solution (Becton Dickenson, Franklin Lakes, NJ, USA), leukocytes were washed twice and suspended in PBS (pH 7.4). Lymphocyte and monocyte H_2O_2 production was measured using a FACS Caliber flow cytometer (Becton Dickinson) according to the method of Bass et al. (56). For specific details see the online data supplement available at http://www.circresaha.org.

PBMC Transcriptome

Total RNA was isolated from purified PBMC using a tri-reagent (Invitrogen, Carlsbad, CA, USA). The gene expression analysis was conducted as previously described (57) using the Affymetrix rat genome U34A chip (Affymetrix, San Diego, CA, USA) probing approximately 7000 known genes and 1000 expressed sequence tags (EST). A total of 6 unoperated/untreated controls, 6 ALDOST obtained at each time point, and 6 ALDOST+Spi obtained at each time point, went into the characterization of transcriptomes. Each sample analyzed on expression array chips consisted of pooled RNA from 3 animals. We compared transcriptomes from untreated controls to samples obtained at wks 1 to 4 of ALDOST to produce a list of genes affected by the treatment. The experiment was repeated and only genes that showed differential expression (≥2-fold) in response to treatment in both of these independent experiments are reported as differentially expressed genes.

Multi-color Flow Cytometric Analysis of Lymphocyte Activation

Heparinized blood was obtained by cardiac puncture and PBMC were isolated by density gradient centrifugation over Histopaque 1077 (Sigma, St. Louis, MO, USA). PBMC were counted, washed twice and resuspendedin Dubelco's PBS (Invitrogen Corporation, Carlsbad, CA, USA) supplemented with 2% FCS. For cell surface labeling, PBMC (9×10^5/sample) were incubated with a cocktail of FITC-labeled, PE-labeled, PercP-labeled and APC-labeled antibodies at 4°C for 20 min, washed, and resuspended in PBS-2% FCS. The mouse anti-rat mAbs used for flow cytometry in this study were as follows: FITC-conjugated G4.18 (anti-

CD3), OX-33 (anti-CD45RA); PE-conjugated OX-18 (anti-MHC Class I/RT1-A); PercP-conjugated OX-8 (anti-CD8) and OX-6 (anti-MHC Class II/RT1-B); APC-conjugated 1F4 (anti-CD3) and OX-35 (anti-CD4) (all from BD Biosciences, San Jose, CA, USA). Parallelsamples of cells were also incubated with Ig isotypic controls (BD Biosciences). Optimal antibody dilutions were determined in preliminary experiments. All samples were immediately analyzed on a FACS Caliber flow cytometer (Becton Dickinson). Fluorescence data from at least30,000 cells (from a lymphocyte gate) were collected for each sample. Off-line analyses of raw data were performed using WinMDI software(J. Trotter, Scripps Institute, La Jolla, CA, USA).

3-Nitrotyrosine in Invading Inflammatory Cells

Expression of oxi/nitrosative stress were studied by immunohistochemical localization of 3-nitrotyrosine. Lymphocytes and macrophages were detected by immunohistochemical assessment using CD4 and ED-1, respectively. Coronal cryostat sections (6 μm) were prepared, air-dried, fixed in 10% buffered formalin for 5 min and washed in PBS for 10 min. Sections were then incubated with primary antibody against 3-nitrotyroxine at a dilution of 1:100 (Upstate Biotech, Waltham, MA, USA) or CD4 at a dilution of 1:50 (Becton Dickinson) or ED-1 at a dilution of 1:140 (Harlan Bioproducts, Indianapolis, IN, USA) in PBS containing 1% BSA for 60 min. Sections were then washed in PBS for 10 min and incubated with IgG-peroxidase conjugated secondary antibody (Sigma) with a dilution of 1:150, washed in PBS for 10 min, incubated with 0.5 mg/mL diaminobenzidine tetrahydrochloride 2-hydrate+0.05% H_2O_2 for 10 min, and rewashed in PBS. Negative control sections were incubated with secondary antibody alone, stained with hematoxylin, dehydrated, mounted, and examined by light microscopy.

Statistics

Results for plasma and cardiac tissue [Mg^{2+}], total PBMC Mg^{2+} and Ca^{2+}, PBMC $[Mg^{2+}]_i$ and $[Ca^{2+}]_i$, and H_2O_2 production by PBMC are expressed as the mean ± standard error of the mean (SEM). Data were analyzed by analysis of variance (ANOVA) and significant differences between groups determined using the Student-Newman-Keuls multiple comparisons test and were considered statistically significant when $p<0.05$.

RESULTS

Animals

During wks 1 and 2 ALDOST, 9- and 10-week-old rats were active, eating and drinking. They were also gaining weight comparable to age-/gender-matched controls (Figure 1). Rats receiving ALDOST plus Spi co-treatment for wks 1 and 2 were also healthy and their body weight was no different from controls (Figure 1). This preclinical stage was followed by the appearance of lethargy and anorexia during wks 3 and 4 ALDOST. During this clinical stage, rats failed to gain weight and their body weight was no longer comparable to controls (Figure 1). On the other hand, animals receiving Spi co-treatment remained healthy, active and gained weight similar to that observed in both control groups (Figure 1).

Systolic blood pressure at wk 1 ALDOST was no different from unoperated/untreated (UO) and uninephrectomized/salt-treated (UN) control groups, but rose gradually thereafter and was significantly greater ($p<0.05$) than controls at wks 3 and 4 (Table 1). Co-treatment with Spi prevented the gradual rise in blood pressure with animals remaining normotensive throughout the 4-wk period of observation (Table 1).

Plasma and Cardiac Tissue Mg^{2+} Concentrations

The concentration of plasma Mg^{2+} at 4 wks ALDOST (1.51±0.10 mg/dL) was no different from UO or UN controls (1.40±0.06 and 1.45±0.15 mg/dL, respectively) and was not altered by co-treatment with Spi (1.74±0.17 mg/dL).

The concentration of Mg^{2+} in cardiac tissue in UO and UN controls was 79.91±9.61 and 80.17 ±9.32 nEq/mg FFDT and remained unchanged at 4 wks ALDOST (75.77±6.34 nEq/mg FFDT).

Total Intracellular Mg^{2+} and Ca^{2+} in PBMC

Total Mg^{2+} in PBMC harvested from untreated controls was 1.45±0.05 μg/mg protein. At wks 1 to 4 ALDOST, this value was found to be increased: 1.63±0.13, 1.85±0.07, 1.68±0.03 and 1.71±0.11 μg/mg protein, respectively.

The total concentration of Ca^{2+} in PBMC obtained from controls was 0.60±0.05 μg/mg protein. PBMC total Ca^{2+} was increased in response to 1–4 wks ALDOST: 0.87±0.03, 0.77±0.08, 0.83 ±0.23 and 1.14±0.11 μg/mg protein, respectively.

Cytosolic Free $[Mg^{2+}]_i$ and $[Ca^{2+}]_i$ in PBMC

No difference in PBMC count was observed between controls and ALDOST, with or without Spi co-treatment, at any weekly time point (data not shown).

Compared to controls and as shown in the left panel of Figure 2, PBMC $[Mg^{2+}]_i$ was significantly ($p<0.05$) reduced at wk 1 ALDOST. At wk 2, ionized $[Mg^{2+}]_i$ levels were again normal and no different from UO or UN controls. Thereafter, $[Mg^{2+}]_i$ was again reduced ($p<0.05$) at wks 3 and 4 ALDOST. Spi co-treatment did not alter these sequential changes in $[Mg^{2+}]_i$ observed with 1–3 wks ALDOST, but $[Mg^{2+}]_i$ was at control levels at wk 4 (left panel, Figure 2).

At wk 1 ALDOST, PBMC $[Ca^{2+}]_i$ was unchanged from controls, but rose progressively thereafter and was greater than both control groups at wks 2, 3 and 4 (right panel, Figure 2). Spi co-treatment abrogated intracellular Ca^{2+} loading during wks 2–4 ALDOST (right panel, Figure 2).

Hydrogen Peroxide Generation by PBMC

At wk 1 of ALDOST, H_2O_2 generation was no different from baseline levels prior to uninephrectomy and to initiating ALDOST (Figure 3). At wk 2 of ALDOST, monocytes (left panel) and lymphocytes (right panel) demonstrated increased H_2O_2 production as compared to baseline and wk 1 values and this was sustained at wks 3 and 4 (Figure 3). Spi co-treatment abrogated increased H_2O_2 generation by both monocytes and lymphocytes at wks 2, 3 and 4 ALDOST (Figure 3).

PBMC Transcriptome

For the analysis of PBMC expressed genes, i.e., their transcriptome, 3 pooled blood samples were obtained from 9 controls while those harvested weekly from rats receiving either ALDOST or co-treatment with Spi were harvested from 24 rats per treatment group with 6 rats at each time point per group. Gene chip array analysis was interrogated and compared for the differential (≥2-fold) expression (either up- or downregulated) of genes related to: shifts in intracellular mono- and divalent cations, Na^+, Mg^{2+} and Ca^{2+}; the presence of oxi/nitrosative stress; and PBMC activation and phenotype.

Relevant to the decline in PBMC $[Mg^{2+}]_i$ seen during wk 1 of the preclinical stage of ALDOST and which was presumably accompanied by Na^+ loading (not measured), we found upregulated

gene expression of an ATPase inhibitor protein (upper left panel, Figure 4) and a Na^+-dependent transporter (lower left panel, Figure 4), which was sustained over 4 wks. Spi co-treatment attenuated these responses. Other upregulated PBMC genes seen during this time frame with ALDOST (not shown) included: somatostatin receptor and Na^+-dependent serotonin transporter while the α_1 isoform of Na^+/K^+-ATPase was downregulated. Spi co-treatment served to attenuate these responses at all time points. We did not find specific genes that only became markedly (>2-fold) up- or downregulated at wks 3 or 4 of ALDOST or which responded in like manner to Spi co-treatment at these time points.

Intracellular Ca^{2+} loading, initially of organelles and subsequently free ionized cytosolic levels, appeared during the preclinical stage of ALDOST and was associated with upregulated expression of an ATP-dependent Ca^{2+} pump (upper right panel, Figure 4) and calmodulin kinase, a Ca^{2+}-dependent protein kinase C-associated kinase (lower right panel, Figure 4). Co-treatment with Spi attenuated these responses. Other Ca^{2+}-related genes that were upregulated during this time period of ALDOST (not shown) included: calgranulin A, a Ca^{2+}-binding chemokine; and proteins involved in intracellular Ca^{2+} binding, such as calgranulin B, lipocortin I and a Ca^{2+}-binding protein. A downregulation in gene expression (not shown) was seen for Ca^{2+}-inhibitable adenylcyclase while FAK-2, a Ca^{2+}-dependent tyrosine kinase, was unchanged from controls. Spi attenuated the response in Ca^{2+} binding protein, but did not alter these other responses at any time point. We did not find specific genes that were first markedly up- or downregulated at wks 3 or 4 of ALDOST or which were similarly altered by Spi co-treatment.

The presence of oxi/nitrosative stress in PBMC throughout 4 wks ALDOST was evidenced by responses in their transcriptome. This included: an early, upregulated expression of oxidative stress-inducible tyrosine phosphatase (not shown); and such antioxidant defenses as Mn^{2+}-superoxide dismutase and L-cysteine oxireductase (upper and lower panels, Figure 5). Inducible nitric oxide synthase was also upregulated (not shown) and is integral to nitric oxide formation that regulates the mitochondrial electron transport chain, a major source of reactive oxygen species. Glutathione peroxidase and reductase, catalase and NADPH oxireductase were not altered. During wks 2–4 ALDOST and accompanying the increased H_2O_2 production by PBMC, we found an activation and iteration in their phenotype. Evidence of early PBMC activation included: upregulated expression of ICAM-1 and integrin-α_1 (upper and lower left panels, Figure 6); cell adhesion regulator; CC chemokine receptor protein; chemokine receptor CCR2; CXC chemokine receptor; interleukin (IL)-1β, its receptor type 2 and accessory protein; and interferon-γ-inducible GTP cyclohydrolase. Spi attenuated these responses. An iteration in PBMC phenotype was suggested by a downregulation in major histocompatibility (MHC) class I molecule together with upregulated expression of MHC class II A–β (upper right panel, Figure 6), IgE binding protein, IgG2b rearranged gene and IgA constant region (not shown). Autoreactivity was evidenced by upregulated gene expression of antibodies to acetylcholine receptors and nerve growth factor and a downregulation to the expression of RT-6.2 (lower right panel, Figure 6), each of which was attenuated by Spi co-treatment.

Lymphocyte Activation

Our transcriptome data suggested ALDOST treatment is accompanied by B cell activation (e.g., increased immunoglobulin gene transcription). At wk 4 we determined the B/T cell ratio in control, ALDOST and Spi co-treated rats by flow cytometry (Figure 7) and found a relative expansion of the B lymphocyte subset in ALDOST rats when compared to UN controls and which was attenuated by Spi. Moreover, MHC Class II-expressing lymphocytes were increased in ALDOST rats at wk 4, consistent with the upregulation of MHC II genes. The increase in MHC Class II-positive cells is also in keeping with the immune activation induced by ALDOST. Indeed, by multi-color flow cytometry, we confirmed that the B cell subset is the

major Class II-expressing population of lymphocytes. Within the $CD3^+$ T cell population, we did not detect differences in the CD4/CD8 ratio among the various treatment groups (data not shown).

3-Nitrotyrosine in Immune Cells Invading the Coronary Vasculature

As reported previously (41,42), the proinflammatory coronary vascular phenotype first appears at wk 4 ALDOST. Peroxynitrite ($OONO^-$) is a potent reactive nitrogen species formed by the reaction of nitric oxide and superoxide. Its short half-life makes detection of $OONO^-$difficult. However, its reaction with stable tyrosine residues forms a stable 3-nitrotyrosine derivative and serves as a marker of nitrosative stress. Immunohistochemical evidence of 3-nitrotyrosine was found in inflammatory cells, including CD4+ lymphocytes, that invaded the coronary vasculature of the right and left heart at wk 4 of ALDOST (see panels A and C, Figure 8). ED-1-positive macrophages were also found to have 3-nitrotyrosine labeling (not shown). Co-treatment with Spi prevented the appearance of 3-nitrotyrosine labeling in cells that invaded intramural coronary arteries (panel B) and attenuated the number of inflammatory cells seen at these sites.

DISCUSSION

Herein we hypothesized that chronic treatment with ALDO and 1% dietary NaCl leads to an iteration in PBMC divalent cation composition which, in turn, accounts for an induction of oxi/nitrosative stress and activation of these immune cells that subsequently invade the intramural coronary vasculature of the right and left heart. We further hypothesized that by abrogating these responses in PBMC divalent cations Spi would be immunomodulatory. Our study led to several major findings.

Beginning with the preclinical stage of ALDOST we found a reduction in PBMC $[Mg^{2+}]_i$ which was significantly lower than levels found in PBMC obtained from either of our two control groups or historical controls reported by others (58). Furthermore, the fall in this biologically active component of intracellular Mg^{2+} seen with ALDOST is in keeping with significantly reduced human lymphocyte $[Mg^{2+}]_i$ found in patients with primary aldosteronism (50). The mechanism responsible for the reduction in $[Mg^{2+}]_i$ is unknown. It could involve an efflux out of the cell, a shift within the cell's compartment, or both. Delva et al. (50) reported a Na^+-dependent, ALDO-mediated reduction in $[Mg^{2+}]_i$ in cultured human lymphocytes and which involved transcription and protein synthesis; thereby a putative Na^+/Mg^{2+} exchange site (59) was implicated. In chicken erythrocytes, Mg^{2+} efflux is dependent on extracellular Na^+ with a stoichiometry of 1 Mg^{2+} coupled to the influx of 2 Na^+ via a Na^+/Mg^{2+} exchanger (60). Cytosolic free $[Mg^{2+}]_i$ represents 0.5–5% of total cellular Mg^{2+} and the remainder is bound to ATP and other phosphometabolites sequestered within such organelles as mitochondria and endoplasmic reticulum (61). At wk 2 ALDOST, PBMC $[Mg^{2+}]_i$ was similar to that seen in our controls. This might reflect homeostatic regulation from these organelles although the appearance of a new PBMC population cannot be ruled out. A decline in PBMC $[Mg^{2+}]_i$ was again seen at wks 3 and 4 of ALDOST. Other explanations accounting for the reduction in $[Mg^{2+}]_i$ need to be considered. PBMC total Mg^{2+} concentration was increased during wks 1–4 ALDOST and likely includes the activation of protein kinase C to promote Mg^{2+} entry and compartmentalization with the opening of mitochondrial permeability transition pores induced by oxi/nitrosative stress and Ca^{2+} loading (62–64). A reduction in organellar Mg^{2+} stores therefore cannot be implicated in the fall of $[Mg^{2+}]_i$. Given that cytosolic free $[Mg^{2+}]_i$ represents such a small fraction of total Mg^{2+} it is not likely that the observed increase in total Mg^{2+} could be attributed to this source. We did not find a reduction in plasma $[Mg^{2+}]$ or a decline in cardiac tissue $[Mg^{2+}]$ with 4 wk ALDOST even though urinary Mg^{2+} excretion (not measured herein) can be enhanced by ALDO (65). We cannot implicate

dietary Mg^{2+} deficiency given that the Mg^{2+} content of our standard chow (20–40 mmol/kg) is in keeping with daily requirements and far greater than that (<2 mmol/kg) needed to induce dietary Mg^{2+} deficiency (66,67). Future studies are planned to address responsible mechanisms.

Mg^{2+} is involved in over 300 enzymatic reactions, including Mg^{2+}-dependent Na^+/K^+-ATPase (59,61). A reduction in the activity of this exchanger leads to a rise in intracellular Na^+ followed by the stoichiometric exchange of 3 Na^+ for 1 Ca^{2+} via a Na^+/Ca^{2+} exchanger (68,69). At wk 1 ALDOST, analysis of PBMC transcriptome revealed upregulated expression of an ATPase inhibitor protein and Na^+-dependent transporter together with a downregulation in α_1 isoform of Na^+/K^+-ATPase and upregulation in ATP-dependent Ca^{2+} pump, each of which persisted during subsequent wks of ALDOST. Spi attenuated these responses. Total intracellular Ca^{2+} was increased throughout the 4-wk period of ALDOST and is likely responsible for the early and persistent induction of oxi/nitrosative stress. PBMC $[Ca^{2+}]_i$ rose at wks 2–4 ALDOST in keeping with the saturation of organellar stores during week 1. ALDO and extracellular Na^+ are each known to upregulate Ca^{2+} uptake in various cells, including lymphocytes (70,71). Furthermore, ALDO reversibly downregulates the activity of a Na^+/Ca^{2+} exchanger, which would inhibit net Ca^{2+} efflux from PBMC (72,73). Collectively, these responses would account for intracellular Ca^{2+} loading, which we observed for both cytosolic free $[Ca^{2+}]_i$ and total Ca^{2+} concentration of PBMC. In both man and experimental animals, chronic mineralocorticoid excess, derived from either endogenous or exogenous sources and inappropriate for dietary Na^+, is associated with a rise in platelet $[Ca^{2+}]_i$ and release of endogenous, circulating ouabain, a Na^+/K^+-ATPase inhibitor, which normalized after surgical ablation (74–78). Na^+–Ca^{2+} exchange is dependent on cell Na^+ and is competitively inhibited by Mg^{2+} (79). A 4 gm NaCl diet in blacks with salt-sensitive hypertension is accompanied by increases in erythrocyte Ca^{2+} and Na^+ concentrations and Ca^{2+}-ATPase activity while $[Mg^{2+}]_i$ and Na^+/K^+-ATPase activity are each reduced (80). Spi co-treatment in our rodent model of ALDOST prevented the rise in $[Ca^{2+}]_i$ that appeared at wks 2–4 of ALDOST suggesting it altered Na^+ delivery to and Na^+/Ca^{2+} exchange in PBMC (81). The fall in $[Mg^{2+}]_i$, which was not prevented by Spi, does not therefore appear to be an absolute prerequisite to PBMC Ca^{2+} loading. However, a reduction in $[Mg^{2+}]_i$, a physiologic antagonist to Ca^{2+} entry, would indirectly elevate $[Ca^{2+}]_i$ (81). ALDO also increases the density of Ca^{2+} current and Ca^{2+} channel expression, responses blunted by Spi (71). Nifedipine, a dihydroperidine Ca^{2+} entry blocker, prevents renovascular lesions that accompany chronic mineralocorticoid excess (82). Thus, our findings implicate Na^+-dependent intracellular Ca^{2+} loading as integral to other events that appeared in PBMC during ALDOST. Increased $[Ca^{2+}]_i$ is an intracellular messenger integral to lymphocyte activation that appears in response to antigen-binding and antigen-presenting cells (83). It has been reported to play a major regulatory role in the generation of reactive oxygen species in chemotactic factor-stimulated neutrophils (81).

Concordant with the rise in intracellular Ca^{2+} was the induction of oxi/nitrosative stress in PBMC as indicated by several lines of evidence. PBMC transcriptome at 1–4 wks ALDOST revealed overexpression of oxidative stress-inducible tyrosine phosphatase and upregulation of enzymes associated with antioxidant defense systems, such as Mn^{2+}-superoxide dismustase (SOD), L-cysteine and NADPH oxireductases, and inducible nitric oxide synthase. In monocytes and lymphocytes obtained from rats receiving ALDOST at 2–4 wks, we found evidence of increased H_2O_2 production suggesting antioxidant defenses in these cells were no longer able to neutralize this stress, as presumably had been the case at wk 1. Persistent oxi/nitrosative stress may have contributed to the appearance of the systemic illness and catabolic state seen in these rats at wks 3–4 ALDOST and which featured lethargy, anorexia and a failure to gain weight. In preventing oxi/nitrosative stress, Spi co-treatment prevented this clinical response. At wk 4 ALDOST we found immunohistochemical localization of 3-nitrotyrosine

in inflammatory cells that invaded intramural coronary arteries. Sun et al. (42) have previously reported the presence of oxi/nitrosative stress in these immune cells that first invade the coronary circulation at 4 wks ALDOST. This included activation of $gp91^{phox}$, a membrane-bound NADPH oxidase subunit, and the RelA subunit of a redox-sensitive nuclear transcription factor-κB, together with a proinflammatory mediator cascade it regulates. This cascade included upregulated mRNA expression of intercellular adhesion molecule (ICAM)-1, monocyte chemoattractant protein (MCP)-1 and tumor necrosis factor (TNF)-α. These cellular and molecular events were not seen when ALDOST was combined with either an antioxidant or Spi. Herein, we report the prevention of the rise in PBMC $[Ca^{2+}]_i$ by Spi co-treatment and this negated the induction of oxi/nitrosative stress in these immune cells that invade the coronary vasculature.

A third finding of our study was the activation of PBMC prior to the appearance of the proinflammatory coronary vascular phenotype seen at wk 4 ALDOST. This occurred in the absence of myocardium-derived antigen given that the heart in our rat model is intact and free of prior injury. This early immunostimulatory state included: 1) B cell activation with increased expression of immunoglobulins; 2) an expansion of the B cell lymphocyte subset; 3) an increase in MHC Class II-expressing lymphocytes; 4) increased expression of ICAM-1, integrin-α_1, CC chemokine receptor protein and receptor CCR_2, CXC chemokine receptor, IL-1β, its receptor type 2 and accessory protein; and 5) inducible interferon-γ. There was also evidence to implicate autoreactivity with increased expression of antibodies to acetylcholine receptors and nerve growth factor and reduced RT-6.2. RT-6, an alloantigenic marker of mature resting T cells, is lost upon activation. Cytotoxic T cells do not display RT-6 and are associated with autoimmunity (84–87). RT-6 exists in at least 2 allelic forms, RT-6.1 and RT-6.2, where RT-6.2 consists of a nonglycosylated 25 and 28 kD form (88). Circulating levels of CC chemokines, including MCP-1, macrophage inflammatory protein (MIP)-1α, and RANTES (Regulated on Activation Normally T cell Expressed and Secreted), are increased particularly in patients with advanced, symptomatic failure at rest (NYHA Class IV) irrespective of its etiologic origins (16). Monocytes and $CD3^+$ lymphocytes (T lymphocytes), obtained from individuals with NYHA Class III and IV failure, have been studied in culture with respect to their release of CC chemokines (16). In response to stimulation of monocytes with LPS or $CD3^+$ lymphocytes with anti-CD3/anti-CD28 monoclonal antibodies, increased release of MIP-1α and MCP-1 was observed for monocytes and increased release of RANTES by $CD3^+$ lymphocytes (vis-à-vis healthy blood donor controls). The effect of serum from these patients on superoxide generation by cultured monocytes harvested from healthy blood donors was also examined (16). Spontaneous and provoked generation of superoxide was enhanced and to an extent related to serum MCP-1 levels and which could be inhibited by neutralizing antibodies to this CC chemokine. Serum levels of CXC chemokines, including IL-8, growth-regulated oncogene (GRO)α and epithelial neutrophil activating peptide (ENA)-78, are also elevated in patients with heart failure and to an extent related to the severity of symptomatic heart failure (17). Furthermore, spontaneous and LPS-stimulated monocytes from these patients release elevated amounts of these CXC chemokines (17). Damås et al. (18) demonstrated upregulated PBMC gene expression (ribonuclease protection assay) for MIP-1α and -1β, IL-8 and their corresponding receptors that include CCR1 and CCR5, CXC chemokine receptor (CXCR)1 and CXCR2, in patients with heart failure of diverse causality. Thus in man with symptomatic heart failure, where salt and water retention and elevated plasma levels of ALDO are expected, as well as in our rodent model of ALDOST, there is evidence of sustained monocyte and lymphocyte activation. Such “runaway inflammation” may contribute to the chronic “cytokine storm” seen with the CHF syndrome. An initial immunostimulatory state that begins during wk 1 ALDOST, based on Na^+-dependent, ALDO-induced activation of PBMC, is sustained and begets an immunopathologic state with cardiac lesions at wk 4. Dietary induced Mg^{2+} deficiency and associated aldosteronism (89,90), is accompanied by: reduced Mg^{2+} and increased Na^+ and Ca^{2+} in lymphocytes (91); evidence of oxi/-nitrosative stress in plasma,

reduced antioxidant reserves in PBMC; elevated PBMC proinflammatory cytokine production at wk 1; and a delayed appearance in cardiac pathology seen at wk 3 (66,67) together with upregulated expression of stress proteins and glutathione transferase in neutrophils and thymocytes (92,93). The appearance of exaggerated immune cell responses seen with Mg^{2+} deficiency, includes superoxide anion production and enhanced $[Ca^{2+}]_i$, which have been attributed to abnormal Ca^{2+} handling (94).

We believe the antigen-independent activation of cellular immunity seen with ALDOST is related to H_2O_2 production and its role as second messenger. Reth (95) has reviewed the evidence implicating H_2O_2 as second messenger capable of antigen mimicry. Redox-regulated proteins include transcription factors that can either prevent (e.g., p53) or stimulate (p50) their transcriptional activity. Other redox-regulated proteins, which we observed in our analysis of PBMC transcriptome, are the protein tyrosine phosphatases. They are rendered inactive by H_2O_2. In lymphocytes, H_2O_2 can be spontaneously generated from superoxide and protons in water or catalyzed by cytosolic SOD. Another source of superoxide is NADPH oxi/reductase. In response to ALDOST we found upregulated expression of both SOD and NADPH oxi/reductase in PBMC transcriptome. Sun et al. (42) found immunohistochemical evidence that the $gp91^{phox}$ subunit of NADPH oxidase was activated in cells invading the intramural coronary vasculature. NADPH oxidase is pertinent to inducible oxi/nitrosative stress in lymphocytes during signal transduction (96). Lymphocytes produce H_2O_2 upon stimulation of their antigen receptor, while immunoglobulins (or antibodies) do not require a particular antigen binding site to incite H_2O_2 production (97–99). Receptors can be activated in a ligand-independent manner when immune cells are treated with H_2O_2. B cell activation leads to antibody production. In patients with heart failure of diverse origins, circulating antibodies to muscarinic M_2-acetylcholine receptors (AchR) have been observed and correlated with the severity of their symptomatic status (100–104). Specific immune responses may be involved in activated PBMC targeting the intramural coronary vasculature and could explain why cardiac lesions of the right and left heart are not seen until wk 4 of ALDOST. Adoptive transfer studies have been planned to address the issues concerning an autoimmune response. However, the need for coronary endothelial cell activation in contributing to this response remains uncertain.

Findings of this study relate to the pathophysiology of chronic cardiac failure in man, where an activation of the circulating RAAS is accompanied by a progressive systemic illness that features oxi/nitrosative stress, lethargy and a catabolic state with wasting. Herein, we found ALDOST in rodents to lead to an early activation of PBMC prior to the appearance of lethargy, anorexia, failure to gain weight and coronary lesions. The prospect of B cell activation and autoreactivity, in the absence of antigen presentation, calls into question their potential for autoimmune-mediated injury that targets the intramural vasculature and leads to a progressive structural remodeling of involved vessels. Functional consequences of antibody interference with AchR seen with ALDOST may include a modulation of parasympathetic control of heart rate and conduction (105), reduced baroreceptor discharge (106), impaired vasodilator reserve to Ach (40,107), and nerve growth factor that maintains the integrity of sympathetic innervation (108). Our observations broaden the paradigm embraced by the concept of a neuroendocrine-immune interface (109,110).

In summary, findings of this study have addressed several gaps in our knowledge. In aldosteronism, PBMC are activated prior to invading the intramural coronary arterial circulation. Activation of these immune cells by intracellular Ca^{2+} loading leads to the induction of oxi/nitrosative stress, including H_2O_2 production, which likely serves as second messenger to mimic antigen-receptor binding and lymphocyte activation. The clinical efficacy of ALDO receptor antagonism in the management of symptomatic heart failure (26,27), where

aldosteronism is expected, may include its ability to modulate this neuroendocrine-immune interface.

Acknowledgments

This work was supported, in part, by NIH R01-DK62403, R24-RR-15373 and R21-DK-55263 (ICG), NHLBI R01-HL67888 (YS), NHLBI R01-HL62229 (KTW) and grants from the UTHSC Center of Excellence in Connective Tissue Diseases to YS and KTW.

References

1. Chen L, Zang Y, Bai B, Zhu M, Zhao B, Hou J, Xin W. Electron spin resonance determination and superoxide dismutase activity in polymorphonuclear leukocytes in congestive heart failure. Can J Cardiol 1992;8:756–760. [PubMed: 1330241]
2. Singh N, Dhalla AK, Seneviratne C, Singal PK. Oxidative stress and heart failure. Mol Cell Biochem 1995;147:77–81. [PubMed: 7494558]
3. Diaz-Velez CR, Garcia-Castineiras S, Mendoza-Ramos E, Hernandez-Lopez E. Increased malondialdehyde in peripheral blood of patients with congestive heart failure. Am Heart J 1996;131:146–152. [PubMed: 8554002]
4. Hill MF, Singal PK. Antioxidant and oxidative stress changes during heart failure subsequent to myocardial infarction in rats. Am J Pathol 1996;148:291–300. [PubMed: 8546218]
5. Keith M, Geranmayegan A, Sole MJ, Kurian R, Robinson A, Omran AS, Jeejeebhoy KN. Increased oxidative stress in patients with congestive heart failure. J Am Coll Cardiol 1998;31:1352–1356. [PubMed: 9581732]
6. Ide T, Tsutsui H, Kinugawa S, Utsumi H, Kang D, Hattori N, Uchida K, Arimura K, Egashira K, Takeshita A. Mitochondrial electron transport complex I is a potential source of oxygen free radicals in the failing myocardium. Circ Res 1999;85:357–363. [PubMed: 10455064]
7. Ide T, Tsutsui H, Kinugawa S, Suematsu N, Hayashidani S, Ichikawa K, Utsumi H, Machida Y, Egashira K, Takeshita A. Direct evidence for increased hydroxyl radicals originating from superoxide in the failing myocardium. Circ Res 2000;86:152–157. [PubMed: 10666410]
8. Sawyer DB, Colucci WS. Mitochondrial oxidative stress in heart failure: “oxygen wastage” revisited. Circ Res 2000;86:119–120. [PubMed: 10666404]
9. Cesselli D, Jakoniuk I, Barlucchi L, Beltrami AP, Hintze TH, Nadal-Ginard B, Kajstura J, Leri A, Anversa P. Oxidative stress-mediated cardiac cell death is a major determinant of ventricular dysfunction and failure in dog dilated cardiomyopathy. Circ Res 2001;89:279–286. [PubMed: 11485979]
10. Hare JM. Oxidative stress and apoptosis in heart failure progression. Circ Res 2001;89:198–200. [PubMed: 11485969]
11. Tsutsui H, Ide T, Hayashidani S, Suematsu N, Shiomi T, Wen J, Nakamura K, Ichikawa K, Utsumi H, Takeshita A. Enhanced generation of reactive oxygen species in the limb skeletal muscles from a murine infarct model of heart failure. Circulation 2001;104:134–136. [PubMed: 11447074]
12. Wiedermann CJ, Beimpold H, Herold M, Knapp E, Braunsteiner H. Increased levels of serum neopterin and decreased production of neutrophil superoxide anions in chronic heart failure with elevated levels of tumor necrosis factor-alpha. J Am Coll Cardiol 1993;22:1897–1901. [PubMed: 8245346]
13. Munger MA, Johnson B, Amber IJ, Callahan KS, Gilbert EM. Circulating concentrations of proinflammatory cytokines in mild or moderate heart failure secondary to ischemic or idiopathic dilated cardiomyopathy. Am J Cardiol 1996;77:723–727. [PubMed: 8651123]
14. Testa M, Yeh M, Lee P, Fanelli R, Loperfido F, Berman JW, LeJemtel TH. Circulating levels of cytokines and their endogenous modulators in patients with mild to severe congestive heart failure due to coronary artery disease or hypertension. J Am Coll Cardiol 1996;28:964–971. [PubMed: 8837575]
15. Torre-Amione G, Kapadia S, Benedict C, Oral H, Young JB, Mann DL. Proinflammatory cytokine levels in patients with depressed left ventricular ejection fraction: a report from the Studies of Left Ventricular Dysfunction (SOLVD). J Am Coll Cardiol 1996;27:1201–1206. [PubMed: 8609343]

16. Aukrust P, Ueland T, Müller F, Andreassen AK, Nordøy I, Aas H, Kjekshus J, Simonsen S, Frøland SS, Gullestad L. Elevated circulating levels of C-C chemokines in patients with congestive heart failure. Circulation 1998;97:1136–1143. [PubMed: 9537339]

17. Damås JK, Gullestad L, Ueland T, Solum NO, Simonsen S, Frøland SS, Aukrust P. CXC-chemokines, a new group of cytokines in congestive heart failure--possible role of platelets and monocytes. Cardiovasc Res 2000;45:428–436. [PubMed: 10728363]

18. Damås JK, Gullestad L, Aass H, Simonsen S, Fjeld JG, Wikeby L, Ueland T, Eiken HG, Frøland SS, Aukrust P. Enhanced gene expression of chemokines and their corresponding receptors in mononuclear blood cells in chronic heart failure--modulatory effect of intravenous immunoglobulin. J Am Coll Cardiol 2001;38:187–193. [PubMed: 11451272]

19. Deswal A, Petersen NJ, Feldman AM, Young JB, White BG, Mann DL. Cytokines and cytokine receptors in advanced heart failure. An analysis of the cytokine database from the Vesnarinone Trial (VEST). Circulation 2001;103:2055–2059. [PubMed: 11319194]

20. Feldman AM, Combes A, Wagner D, Kadakomi T, Kubota T, Li YY, McTiernan C. The role of tumor necrosis factor in the pathophysiology of heart failure. J Am Coll Cardiol 2000;35:537–544. [PubMed: 10716453]

21. Yndestad A, Damås JK, Eiken HG, Holm T, Haug T, Simonsen S, Frøland SS, Gullestad L, Aukrust P. Increased gene expression of tumor necrosis factor superfamily ligands in peripheral blood mononuclear cells during chronic heart failure. Cardiovasc Res 2002;54:175–182. [PubMed: 12062373]

22. Anker SD, Chua TP, Ponikowski P, Harrington D, Swan JW, Kox WJ, Poole-Wilson PA, Coats AJS. Hormonal changes and catabolic/anabolic imbalance in chronic heart failure and their importance for cardiac cachexia. Circulation 1997;96:526–534. [PubMed: 9244221]

23. The SOLVD Investigators. Effect of enalapril on survival in patients with reduced left ventricular ejection fractions and congestive heart failure. N Engl J Med 1991;325:293–302. [PubMed: 2057034]

24. The SOLVD Investigators. Effect of enalapril on mortality and the development of heart failure in asymptomatic patients with reduced left ventricular ejection fractions. N Engl J Med 1992;327:685–691. [PubMed: 1463530]

25. St John Sutton M, Pfeffer MA, Moye L, Plappert T, Rouleau JL, Lamas G, Rouleau J, Parker JO, Arnold MO, Sussex B, Braunwald E. Cardiovascular death and left ventricular remodeling two years after myocardial infarction: baseline predictors and impact of long-term use of captopril: information from the Survival and Ventricular Enlargement (SAVE) trial. Circulation 1997;96:3294–3299. [PubMed: 9396419]

26. Pitt B, Zannad F, Remme WJ, Cody R, Castaigne A, Perez A, Palensky J, Wittes W. The effect of spironolactone on morbidity and mortality in patients with severe heart failure. Randomized Aldactone Evaluation Study Investigators. N Engl J Med 1999;341:709–717. [PubMed: 10471456]

27. Pitt B, Remme W, Zannad F, Neaton J, Martinez F, Roniker B, Bittman R, Hurley S, Kleiman J, Gatlin M. Eplerenone, a selective aldosterone blocker, in patients with left ventricular dysfunction after myocardial infarction. N Engl J Med 2003;348:1309–1321. [PubMed: 12668699]

28. Brilla CG, Pick R, Tan LB, Janicki JS, Weber KT. Remodeling of the rat right and left ventricle in experimental hypertension. Circ Res 1990;67:1355–1364. [PubMed: 1700933]

29. Everett AD, Tufro-McReddie A, Fisher A, Gomez RA. Angiotensin receptor regulates cardiac hypertrophy and transforming growth factor-β_1 expression. Hypertension 1994;23:587–592. [PubMed: 8175166]

30. Sun Y, Ramires FJA, Weber KT. Fibrosis of atria and great vessels in response to angiotensin II or aldosterone infusion. Cardiovasc Res 1997;35:138–147. [PubMed: 9302358]

31. Selye H, Hall CE. Production of nephrosclerosis and cardiac hypertrophy in the rat by desoxycorticosterone acetate overdosage. Am Heart J 1944;27:338–344.

32. Selye H. The general adaptation syndrome and the diseases of adaptation. J Clin Endocrinol 1946;6:117–230.

33. Selye H, Stone H, Timiras PS, Schaffenburg C. Influence of sodium chloride upon the actions of desoxycorticosterone acetate. Am Heart J 1949;37:1009–1016. [PubMed: 18149962]

34. Masson GMC, Mikasa A, Yasuda H. Experimental vascular disease elicited by aldosterone and renin. Endocrinology 1962;71:505–512. [PubMed: 14470949]

35. Selye H. Protection by a steroid-spironolactone against certain types of cardiac necroses. Proc Soc Exp Biol Med 1960;104:212–213. [PubMed: 14444794]
36. Hall CE, Hall O. Hypertension and hypersalimentation. I. Aldosterone hypertension. Lab Invest 1965;14:285–294. [PubMed: 14283730]
37. Sun Y, Zhang J, Zhang JQ, Ramires FJA. Local angiotensin II and transforming growth factor-β1 in renal fibrosis of rats. Hypertension 2000;35:1078–1084. [PubMed: 10818068]
38. Rocha R, Chander PN, Zuckerman A, Stier CT Jr. Role of aldosterone in renal vascular injury in stroke-prone hypertensive rats. Hypertension 1999;33:232–237. [PubMed: 9931110]
39. Rocha R, Stier CT Jr, Kifor I, Ochoa-Maya MR, Rennke HG, Williams GH, Adler GK. Aldosterone: a mediator of myocardial necrosis and renal arteriopathy. Endocrinology 2000;141:3871–3878. [PubMed: 11014244]
40. Virdis A, Neves MF, Amiri F, Viel E, Touyz RM, Schiffrin EL. Spironolactone improves angiotensin-induced vascular changes and oxidative stress. Hypertension 2002;40:504–510. [PubMed: 12364354]
41. Campbell SE, Janicki JS, Weber KT. Temporal differences in fibroblast proliferation and phenotype expression in response to chronic administration of angiotensin II or aldosterone. J Mol Cell Cardiol 1995;27:1545–1560. [PubMed: 8523418]
42. Sun Y, Zhang J, Lu L, Chen SS, Quinn MT, Weber KT. Aldosterone-induced inflammation in the rat heart. Role of oxidative stress. Am J Pathol 2002;161:1773–1781. [PubMed: 12414524]
43. Rocha R, Rudolph AE, Frierdich GE, Nachowiak DA, Kekec BK, Blomme EA, McMahon EG, Delyani JA. Aldosterone induces a vascular inflammatory phenotype in the rat heart. Am J Physiol 2002;283:H1802–H1810.
44. Brilla CG, Weber KT. Mineralocorticoid excess, dietary sodium and myocardial fibrosis. J Lab Clin Med 1992;120:893–901. [PubMed: 1453111]
45. Brilla CG, Matsubara LS, Weber KT. Anti-aldosterone treatment and the prevention of myocardial fibrosis in primary and secondary hyperaldosteronism. J Mol Cell Cardiol 1993;25:563–575. [PubMed: 8377216]
46. Robert V, Van Thiem N, Cheav SL, Mouas C, Swynghedauw B, Delcayre C. Increased cardiac types I and III collagen mRNAs in aldosterone-salt hypertension. Hypertension 1994;24:30–36. [PubMed: 8021005]
47. Young M, Fullerton M, Dilley R, Funder J. Mineralocorticoids, hypertension, and cardiac fibrosis. J Clin Invest 1994;93:2578–2583. [PubMed: 8200995]
48. Young M, Head G, Funder J. Determinants of cardiac fibrosis in experimental hypermineralocorticoid states. Am J Physiol 1995;269:E657–E662. [PubMed: 7485478]
49. Armanini D, Strasser T, Weber PC. Characterization of aldosterone binding sites in circulating human mononuclear leukocytes. Am J Physiol 1985;248:E388–E390. [PubMed: 3156509]
50. Delva P, Pastori C, Degan M, Montesi G, Brazzarola P, Lechi A. Intralymphocyte free magnesium in patients with primary aldosteronism: aldosterone and lymphocyte magnesium homeostasis. Hypertension 2000;35:113–117. [PubMed: 10642284]
51. Bhattacharya SK. Simultaneous determination of calcium and magnesium in human blood serum by atomic absorption spectrophotometer. Anal Lett 1977;10:817–830.
52. Bhattacharya SK, Williams JC, Palmieri GMA. Determination of calcium and magnesium in cardiac and skeletal muscles by atomic absorption spectroscopy using stoichiometric nitrous oxide-acetylene flame. Anal Lett 1979;12:1451–1475.
53. Bhattacharya SK, Johnson PL, Thakar JH. Reversal of impaired oxidative phosphorylation and calcium overloading in the skeletal muscle mitochondria of CHF-146 dystrophic hamsters. Mol Chem Neuropathol 1998;34:53–77. [PubMed: 9778646]
54. Smith PK, Krohn RI, Hermanson GT, Mallia AK, Gartner FH, Provenzano MD, Fujimoto EK, Goeke NM, Olson BJ, Klenk DC. Measurement of protein using bicinchoninic acid. Anal Biochem 1985;150:76–85. [PubMed: 3843705]
55. Gerling IC, Sun Y, Ahokas RA, Wodi LA, Bhattacharya SK, Warrington KJ, Postlethwaite AE, Weber KT. Aldosteronism. An immunostimulatory state precedes the proinflammatory/fibrogenic cardiac phenotype. Am J Physiol Heart Circ Physiol 2003;285:H813–H821. [PubMed: 12860567]

56. Bass DA, Parce JW, Dechatelet LR, Szejda P, Seeds MC, Thomas M. Flow cytometric studies of oxidative product formation by neutrophils: a graded response to membrane stimulation. J Immunol 1983;130:1910–1917. [PubMed: 6833755]
57. Gerling IC, Sun Y, Ahokas RA, Wodi LA, Bhattacharya SK, Warrington KJ, Postlethwaite AE, Weber KT. Aldosteronism. an immunostimulatory state precedes the proinflammatory/fibrogenic cardiac phenotype. Am J Physiol Heart Circ Physiol 2003;285:H813–H821. [PubMed: 12860567]
58. Sasaki N, Oshima T, Matsuura H, Yoshimura M, Yashiki M, Higashi Y, Ishioka N, Nakano Y, Kojima R, Kambe M, Kajiyama G. Lack of effect of transmembrane gradient of magnesium and sodium on regulation of cytosolic free magnesium concentration in rat lymphocytes. Biochim Biophys Acta 1997;1329:169–173. [PubMed: 9370254]
59. Romani AM, Scarpa A. Regulation of cellular magnesium. Front Biosci 2000;5:D720–D734. [PubMed: 10922296]
60. Gunther T, Vormann J, Forster R. Regulation of intracellular magnesium by Mg^{2+} efflux. Biochem Biophys Res Commun 1984;119:124–131. [PubMed: 6422934]
61. Swaminathan R. Disorders of magnesium metabolism. J Int Fed Clin Chem 1999;11(2):10–18.
62. Weiss JN, Korge P, Honda HM, Ping P. Role of the mitochondrial permeability transition in myocardial disease. Circ Res 2003;93:292–301. [PubMed: 12933700]
63. Romani A, Marfella C, Scarpa A. Regulation of Mg^{2+} uptake in isolated rat myocytes and hepatocytes by protein kinase C. FEBS Lett 1992;296:135–40. [PubMed: 1310287]
64. Romani A, Marfella C, Scarpa A. Regulation of magnesium uptake and release in the heart and in isolated ventricular myocytes. Circ Res 1993;72:1139–1148. [PubMed: 8495544]
65. Horton R, Biglieri EG. Effect of aldosterone on the metabolism of magnesium. J Clin Endocrinol Metab 1962;22:1187–1192. [PubMed: 13964048]
66. Weglicki WB, Mak IT, Phillips TM. Blockade of cardiac inflammation in Mg^{2+} deficiency by substance P receptor inhibition. Circ Res 1994;74:1009–1013. [PubMed: 7512452]
67. Weglicki WB, Mak IT, Stafford RE, Dickens BF, Cassidy MM, Phillips TM. Neurogenic peptides and the cardiomyopathy of magnesium-deficiency: effects of substance P-receptor inhibition. Mol Cell Biochem 1994;130:103–109. [PubMed: 8028589]
68. Philipson KD, Nicoll DA. Sodium-calcium exchange: a molecular perspective. Annu Rev Physiol 2000;62:111–133. [PubMed: 10845086]
69. Blaustein MP. Sodium ions, calcium ions, blood pressure regulation, and hypertension: a reassessment and a hypothesis. Am J Physiol 1977;232:C165–C173. [PubMed: 324293]
70. Ueda T. Na^{+}-Ca^{2+} exchange activity in rabbit lymphocyte plasma membranes. Biochim Biophys Acta 1983;734:342–346. [PubMed: 6615836]
71. Bénitah JP, Vassort G. Aldosterone upregulates Ca^{2+} current in adult rat cardiomyocytes. Circ Res 1999;85:1139–1145. [PubMed: 10590240]
72. Wehling M, Käsmayr J, Theisen K. Aldosterone influences free intracellular calcium in human mononuclear leukocytes in vitro. Cell Calcium 1990;11:565–571. [PubMed: 2285925]
73. Smith L, Smith JB. Regulation of sodium-calcium exchanger by glucocorticoids and growth factors in vascular smooth muscle. J Biol Chem 1994;269:27527–27531. [PubMed: 7961668]
74. Rossi G, Manunta P, Hamlyn JM, Pavan E, De Toni R, Semplicini A, Pessina AC. Immunoreactive endogenous ouabain in primary aldosteronism and essential hypertension: relationship with plasma renin, aldosterone and blood pressure levels. J Hypertens 1995;13:1181–1191. [PubMed: 8586810]
75. Brock TA, Smith JB, Overbeck HW. Relationship of vascular sodium-potassium pump activity to intracellular sodium in hypertensive rats. Hypertension 1982;4(Suppl II):II-43–II-48.
76. Haller H, Thiede M, Lenz T, Lüdersdorf M, Harwig S, Distler A, Philipp T. Intracellular free calcium and ionized plasma calcium during mineralocorticoid-induced blood pressure increase in man. J Hypertens Suppl 1985;3(Suppl 3):S41–S43. [PubMed: 2856752]
77. Kh R, Khullar M, Kashyap M, Pandhi P, Uppal R. Effect of oral magnesium supplementation on blood pressure, platelet aggregation and calcium handling in deoxycorticosterone acetate induced hypertension in rats. J Hypertens 2000;18:919–926. [PubMed: 10930190]

78. Haller H, Thiede M, Lenz T, Lüdersdorf M, Harwig S, Distler A, Philipp T. Intracellular free calcium and ionized plasma calcium during mineralocorticoid-induced blood pressure increase in man. J Hypertens Suppl 1985;3(Suppl 3):S41–S43. [PubMed: 2856752]
79. Lyu RM, Smith L, Smith JB. Sodium-calcium exchange in renal epithelial cells: dependence on cell sodium and competitive inhibition by magnesium. J Membr Biol 1991;124:73–83. [PubMed: 1662727]
80. Zemel MB, Kraniak J, Standley PR, Sowers JR. Erythrocyte cation metabolism in salt-sensitive hypertensive blacks as affected by dietary sodium and calcium. Am J Hypertens 1988;1:386–392. [PubMed: 2850820]
81. Simchowitz L, Foy MA, Cragoe EJ Jr. A role for Na^+/Ca^{2+} exchange in the generation of superoxide radicals by human neutrophils. J Biol Chem 1990;265:13449–13456. [PubMed: 2166029]
82. Dworkin LD, Levin RI, Benstein JA, Parker M, Ullian ME, Kim Y, Feiner HD. Effects of nifedipine and enalapril on glomerular injury in rats with deoxycorticosterone-salt hypertension. Am J Physiol 1990;259:F598–F604. [PubMed: 2221099]
83. Nisbet-Brown E, Cheung RK, Lee JW, Gelfand EW. Antigen-dependent increase in cytosolic free calcium in specific human T-lymphocyte clones. Nature 1985;316:545–547. [PubMed: 3875796]
84. Kalsi JK, Ravirajan CT, Wiloch-Winska H, Blanco F, Longhurst CM, Williams W, Chapman C, Hillson J, Youniou P, Latchman D, Isenberg DA. Analysis of three new idiotypes on human monoclonal autoantibodies. Lupus 1995;4:375–389. [PubMed: 8563732]
85. Moore WV, Chu W, Tong PY, Hess D, Benjamin C, Khalili J, Kover K. Prevention of autoimmune diabetes in the DRBB rat by CD40/154 blockade. J Autoimmun 2002;19:139–145. [PubMed: 12419284]
86. Thiele HG, Haag F. The RT6 system of the rat: developmental, molecular and functional aspects. Immunol Rev 2001;184:96–108. [PubMed: 12086324]
87. Greiner DL, Mordes JP, Handler ES, Angelillo M, Nakamura N, Rossini AA. Depletion of RT6.1+ T lymphocytes induces diabetes in resistant biobreeding/Worcester (BB/W) rats. J Exp Med 1987;166:461–475. [PubMed: 3496416]
88. Thiele HG. Rat Thy-1 antigen and its relation to RT-6. Immunol Ser 1989;45:149–170. [PubMed: 2577316]
89. Ginn HE, Cade R, McCallum T, Fregley M. Aldosterone secretion in magnesium-deficient rats. Endocrinology 1967;80:969–971. [PubMed: 6023564]
90. Solounias BM, Schwartz R. The effect of magnesium deficiency on serum aldosterone in rats fed two levels of sodium. Life Sci 1975;17:1211–1217. [PubMed: 1196006]
91. Ryan MF, Ryan MP. Lymphocyte electrolyte alterations during magnesium deficiency in the rat. Ir J Med Sci 1979;148:108–109.
92. Bussière FI, Zimowska W, Gueux E, Rayssiguier Y, Mazur A. Stress protein expression cDNA array study supports activation of neutrophils during acute magnesium deficiency in rats. Magnes Res 2002;15:37–42. [PubMed: 12030422]
93. Petrault I, Zimowska W, Mathieu J, Bayle D, Rock E, Favier A, Rayssiguier Y, Mazur A. Changes in gene expression in rat thymocytes identified by cDNA array support the occurrence of oxidative stress in early magnesium deficiency. Biochim Biophys Acta 2002;1586:92–98. [PubMed: 11781153]
94. Malpuech-Brugere C, Rock E, Astier C, Nowacki W, Mazur A, Rayssiguier Y. Exacerbated immune stress response during experimental magnesium deficiency results from abnormal cell calcium homeostasis. Life Sci 1998;63:1815–1822. [PubMed: 9820125]
95. Reth M. Hydrogen peroxide as second messenger in lymphocyte activation. Nat Immunol 2002;3:1129–1134. [PubMed: 12447370]
96. Babior BM, Lambeth JD, Nauseef W. The neutrophil NADPH oxidase. Arch Biochem Biophys 2002;397:342–324. [PubMed: 11795892]
97. Devadas S, Zaritskaya L, Rhee SG, Oberley L, Williams MS. Discrete generation of superoxide and hydrogen peroxide by T cell receptor stimulation: selective regulation of mitogen-activated protein kinase activation and Fas ligand expression. J Exp Med 2002;195:59–70. [PubMed: 11781366]
98. Wentworth AD, Jones LH, Wentworth P Jr, Janda KD, Lerner RA. Antibodies have the intrinsic capacity to destroy antigens. Proc Natl Acad Sci U S A 2000;97:10930–10935. [PubMed: 11005865]

99. Finkel T. Signal transduction by reactive oxygen species in non-phagocytic cells. J Leukoc Biol 1999;65:337–340. [PubMed: 10080536]
100. Fu LX, Magnusson Y, Bergh CH, Liljeqvist JA, Waagstein F, Hjalmarson A, Hoebeke J. Localization of a functional autoimmune epitope on the muscarinic acetylcholine receptor-2 in patients with idiopathic dilated cardiomyopathy. J Clin Invest 1993;91:1964–1968. [PubMed: 7683693]
101. Zhang L, Hu D, Li J, Wu Y, Liu X, Yang X. Autoantibodies against the myocardial β_1-adrenergic and M_2-muscarinic receptors in patients with congestive heart failure. Chin Med J (Engl) 2002;115:1127–1131. [PubMed: 12215275]
102. Liu HR, Zhao RR, Jiao XY, Wang YY, Fu M. Relationship of myocardial remodeling to the genesis of serum autoantibodies to cardiac $beta_1$-adrenoceptors and muscarinic type 2 acetylcholine receptors in rats. J Am Coll Cardiol 2002;39:1866–1873. [PubMed: 12039504]
103. Fu ML, Hoebeke J, Matsui S, Matoba M, Magnusson Y, Hedner T, Herlitz H, Hjalmarson A. Autoantibodies against cardiac G-protein-coupled receptors define different populations with cardiomyopathies but not with hypertension. Clin Immunol Immunopathol 1994;72:15–20. [PubMed: 8020188]
104. Matsui S, Fu ML, Shimizu M, Fukuoka T, Teraoka K, Takekoshi N, Murakami E, Hjalmarson A. Dilated cardiomyopathy defines serum autoantibodies against G-protein-coupled cardiovascular receptors. Autoimmunity 1995;21:85–88. [PubMed: 8679906]
105. Wang H, Han H, Zhang L, Shi H, Schram G, Nattel S, Wang Z. Expression of multiple subtypes of muscarinic receptors and cellular distribution in the human heart. Mol Pharmacol 2001;59:1029–1036. [PubMed: 11306684]
106. Wang W. Chronic administration of aldosterone depresses baroreceptor reflex function in the dog. Hypertension 1994;24:571–575. [PubMed: 7960015]
107. Farquharson CA, Struthers AD. Spironolactone increases nitric oxide bioactivity, improves endothelial vasodilator dysfunction, and suppresses vascular angiotensin I/angiotensin II conversion in patients with chronic heart failure. Circulation 2000;101:594–597. [PubMed: 10673249]
108. Gorin PD, Johnson EM Jr. Effects of long-term nerve growth factor deprivation on the nervous system of the adult rat: an experimental autoimmune approach. Brain Res 1980;198:27–42. [PubMed: 6105903]
109. Melmed S. The immuno-neuroendocrine interface. J Clin Invest 2001;108:1563–1566. [PubMed: 11733548]
110. Webster JI, Tonelli L, Sternberg EM. Neuroendocrine regulation of immunity. Annu Rev Immunol 2002;20:125–163. [PubMed: 11861600]

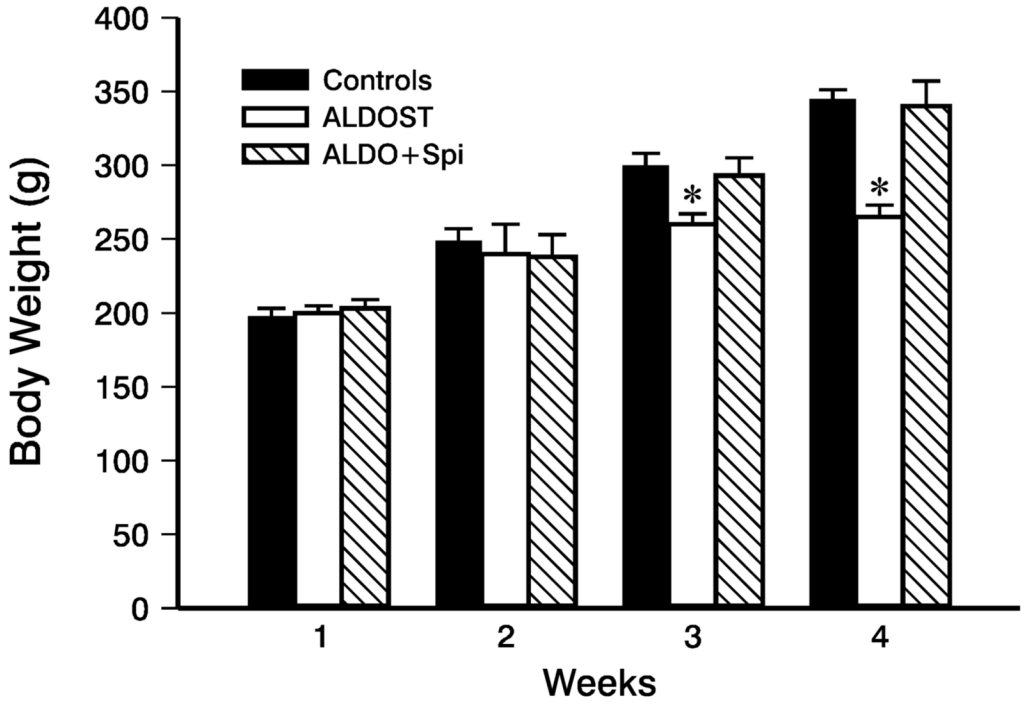

Figure 1.

Body weight for age-/gender-matched controls and that monitored weekly over 4 wks in uninephrectomized rats receiving aldosterone plus a 1% NaCl diet (ALDOST) and ALDOST plus Spi (ALDO+Spi). Spi co-treatment prevented the failure to gain weight seen with ALDOST at wks 3 and 4. *p<0.05 vs. controls; mean±SEM.

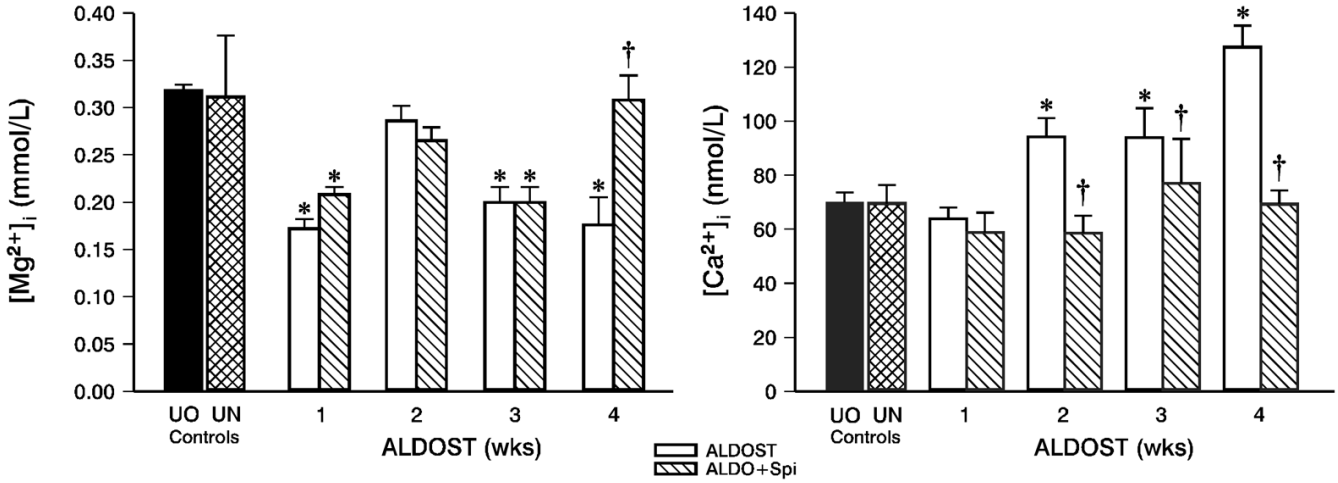

Figure 2.

Cytosolic free $[Mg^{2+}]_i$ (left panel) and $[Ca^{2+}]_i$ (right panel) in peripheral blood mononuclear cells (PBMC) over the course of 4 wks with either ALDOST or ALDO+Spi. Unoperated/-untreated (UO) controls and uninephrectomized rats receiving 1% NaCl (UN) controls. *$p<0.05$ vs. controls; $^{\dagger}p<0.05$ vs. ALDOST; mean±SEM. See text.

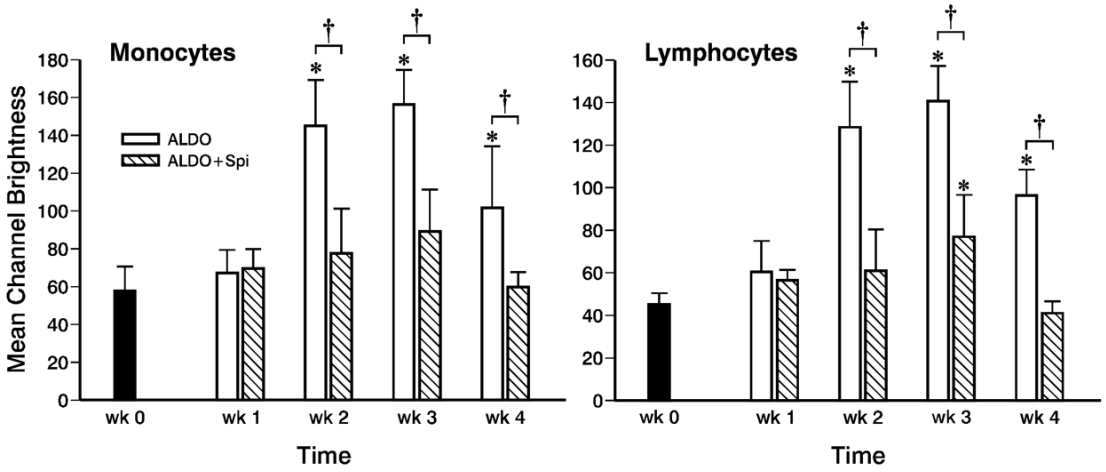

Figure 3.

A longitudinal assessment of H_2O_2 production by circulating monocytes (left panel) and lymphocytes (right panel) obtained serially from the same animals at baseline (wk 0), prior to treatment, and weekly during either ALDOST or ALDO+Spi. H_2O_2 production by flow cytometry, expressed as mean channel brightness, was significantly increased at wks 2, 3 and 4 of ALDOST. Spi co-treatment either prevented (monocytes) or attenuated (lymphocytes) this rise in H_2O_2 production in these cells. *p<0.05 vs. wk 0; $^{\dagger}p$<0.05 vs. Spi; mean±SD.

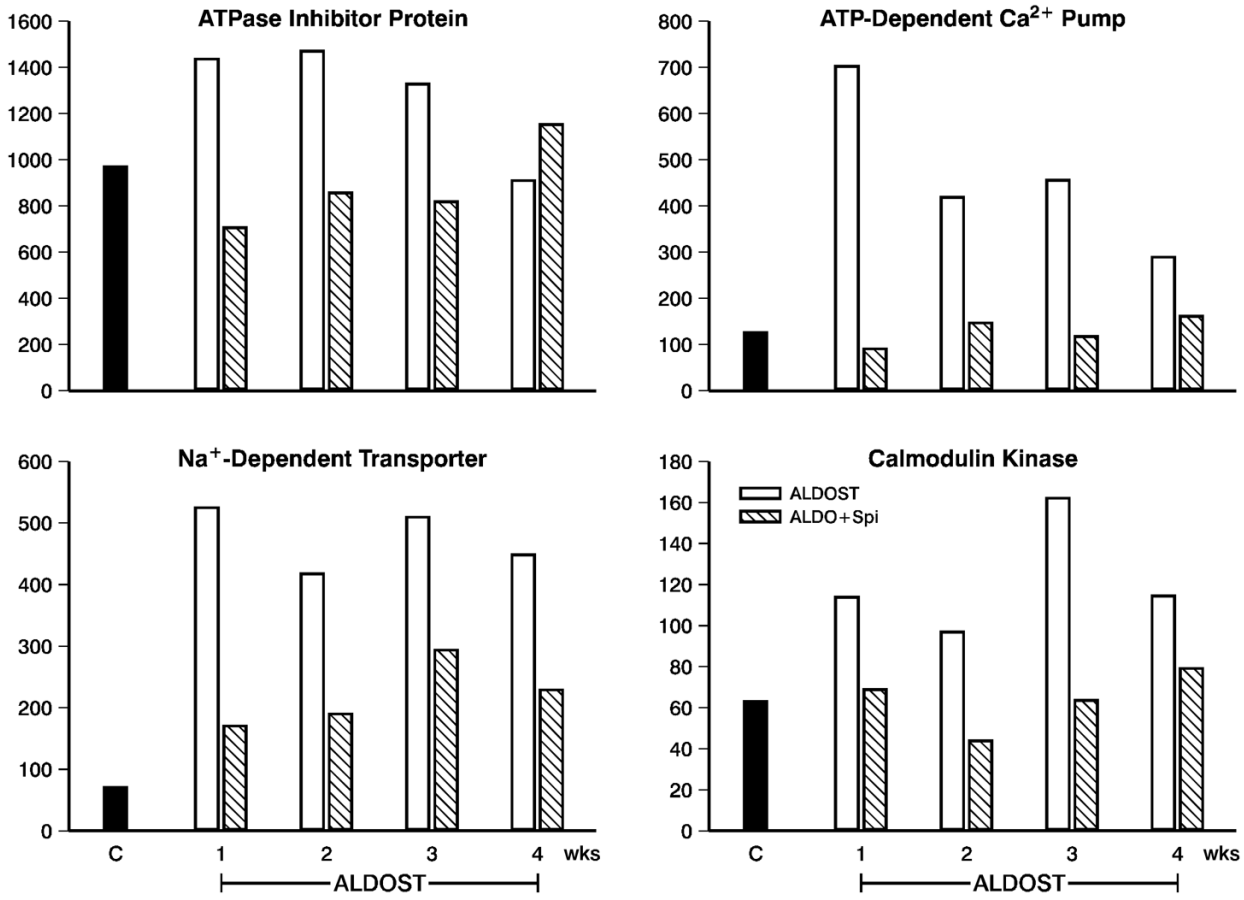

Figure 4.

Gene chip array data obtained in PBMC obtained from 3 pooled samples in controls (n=9) and weekly from rats with ALDOST (n=6) and the combination of ALDO+Spi (n=6). Shown are responses pertaining to shifts in $[Mg^{2+}]_i$ and $[Ca^{2+}]_i$. They include: an upregulation of-ATPase inhibitor protein (upper left) and Na^+-dependent transporter (lower left); and an upregulation of ATP-dependent Ca^{2+} pump (upper right) and calmodulin kinase (lower right). See text.

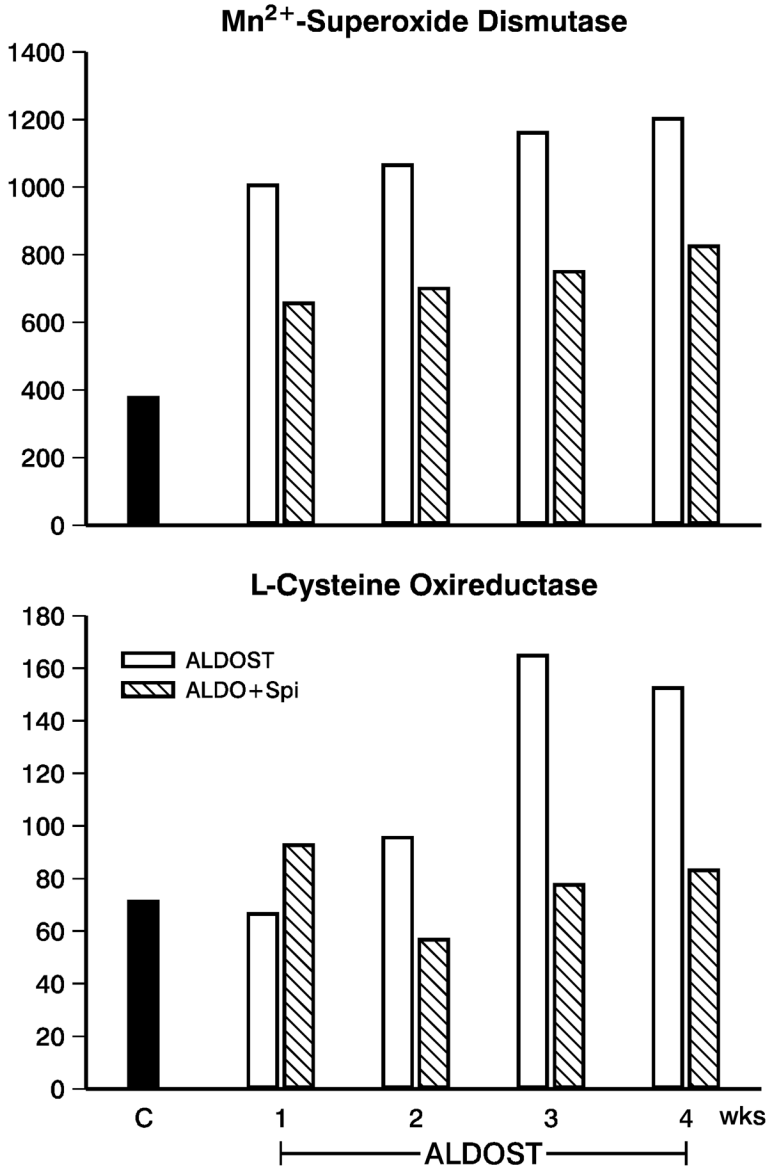

Figure 5.

Transcriptome data in PBMC obtained from 3 pooled samples obtained from controls (n=9) and weekly from rats receiving ALDOST (n=6) and co-treatment with Spi (n=6). Shown are responses which relate to appearance of oxi/nitrosative stress in these cells. These include: the upregulated expression of Mn^{2+}-superoxide dismutase (SOD) (upper panel) and L-cysteine oxireductase (lower panel). See text.

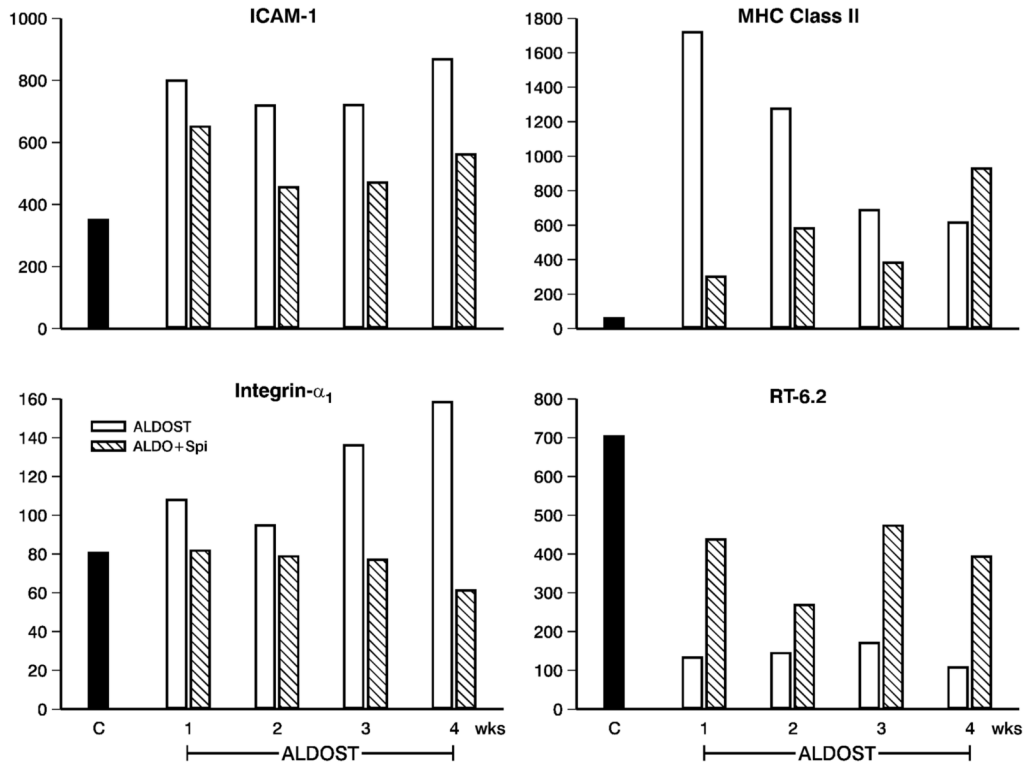

Figure 6.
PBMC transcriptome data (expressed genes) obtained from 3 pooled samples in controls (n=9) and weekly from rats with ALDOST (n=6) and co-treatment with Spi (n=6). Shown are data pertaining to PBMC activation and altered phenotype. These include: the upregulated expression of intercellular adhesion molecule (ICAM)-1 (upper left), integrin-α_1 (lower left) and major histocompatibility (MHC) class II (upper right); and the downregulation of RT-6.2 (lower right). See text.

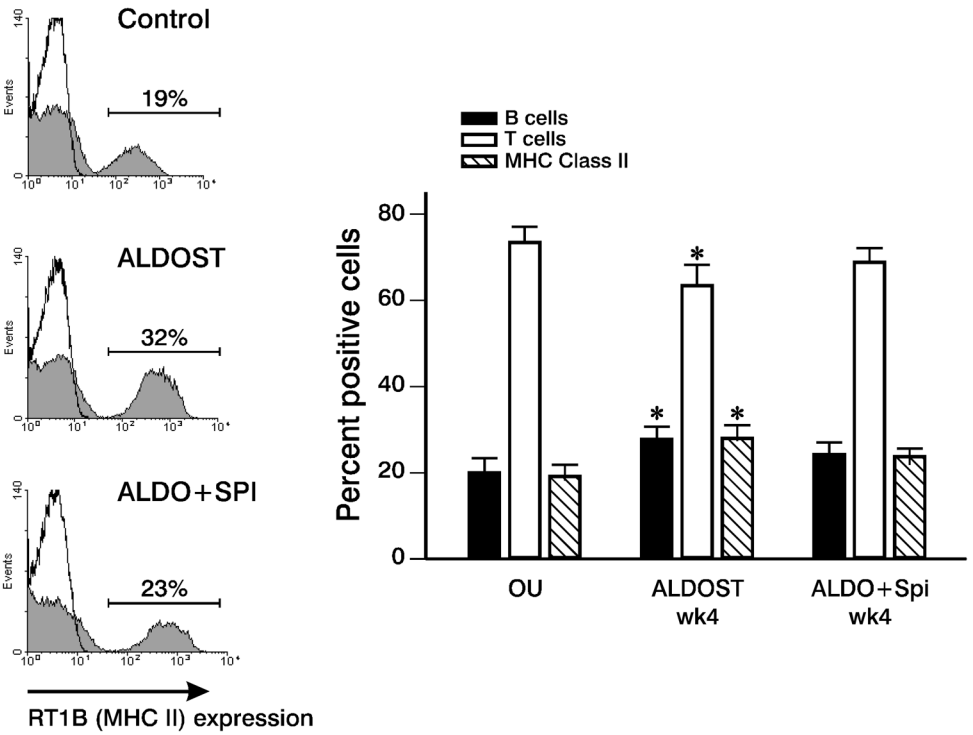

Figure 7.

B lymphocyte activation with ALDOST treatment. The frequency of B cell, T cell and MHC Class II-expressing cell populations in rat PBMC were determined by flow cytometry. Representative data of 5 experiments are shown on the left for MHC Class II expression (shaded area) in control, ALDOST and ALDO+Spi rats. Solid line represents staining with isotype control antibody. On the right, a significant increase in the mean percentage of B cells and MHC Class II-expressing cells and concomitant decrease in T cell percentage occurred in ALDOST rats compared with control animals ($p \leq 0.05$, ANOVA; mean±SEM). This effect was attenuated in ALDO+Spi-treated rats.

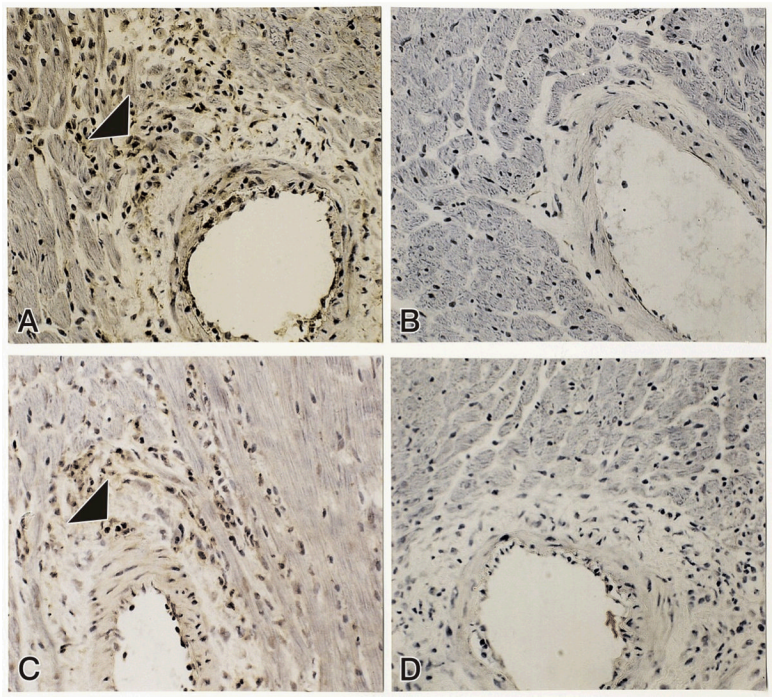

Figure 8.

As detected by immunohistochemistry, inflammatory cells located in the perivascular space of intramural coronary arteries express 3-nitrotyrosine in rats receiving 4 wks ALDOST (panel A, arrowhead). Spi blocked 3-nitrotyrosine expression (panel B) and reduced the number of cells found at these sites. Panel C shows CD4-positive lymphocytes (arrowhead) located in the perivascular space at 4 wks ALDOST. Panel D is a negative control for 3-nitrotyrosine and CD4 staining. 280× magnification.

Table 1

Weekly blood pressure in controls and in ALDOST and ALDO+Spi groups.

	Week 1	Week 2	Week 3	Week 4
UO	119±6	122±8	120±7	118±10
UN	117±5	124±6	118±10	121±9
ALDOST	121±7	127±7	145±10*	187±13*
ALDO+Spi	123±7	126±9	125±12	131±10

* $p<0.05$ vs. controls; mean±SEM